

Epitaxial MgO layer for low-resistance and coupling-free magnetic tunnel junctions

E. Popova,^{a)} J. Faure-Vincent, C. Tiusan, C. Bellouard, H. Fischer, M. Hehn, F. Montaigne, M. Alnot, S. Andrieu, and A. Schuhl
LPM, UHP-CNRS, BP 239, 54506 Vandoeuvre lès Nancy Cedex, France

E. Snoeck
CEMES-CNRS, 29 rue J. Marvig, BP 4347, 31055 Toulouse Cedex, France

V. da Costa
IPCMS, 23 rue du Loess, 67037, Strasbourg Cedex, France

(Received 8 March 2002; accepted for publication 9 June 2002)

Epitaxially grown magnetic tunnel junctions MgO(100)/Fe/MgO/Fe/Co/Pd have been elaborated by molecular beam epitaxy, with insulating layer thickness down to 0.8 nm. The continuity of this layer was checked at different spatial scales by means of morphological (high resolution transmission electronic microscopy), electric (local impedance), and magnetic (magnetoresistance and hysteresis loop) measurements. These junctions show a low resistance ($4 \text{ k}\Omega \mu\text{m}^2$), tunnel magnetoresistance up to 17%, and a very small interlayer magnetic coupling. © 2002 American Institute of Physics. [DOI: 10.1063/1.1498153]

Due to their large potential implication in spin dependent devices, magnetic tunnel junctions (MTJ) have been widely studied during the last decade. Usual MTJ systems, using mainly an Al_2O_3 insulating barrier, present, however, resistance too high for the large application in high density magnetic random access memories (MRAM).¹ The resistance of MTJ can be reduced significantly by decreasing the insulating layer thickness. Recently, tunnel magnetoresistance (TMR) and low resistance have been observed in MTJ with an insulating barrier below 1 nm.^{2,3} However, for such a thin layer, the coupling between the magnetic electrodes of the MTJ increases strongly, affecting the performance of the devices. It is possible to solve this problem by tailoring the stray field of the hard magnetic layer, introducing complex architecture such as an artificial ferrimagnet.⁴ In this letter, we show that the solution can also be found, in a simpler way, by using a molecular beam epitaxy (MBE) for ultrathin multilayer structure growth. We report here on the elaboration and magnetotransport characterization of single crystal MgO(100)/Fe/MgO/Fe/Co/Pd junctions. The epitaxy of metal/insulator superlattice MgO(100)/Fe is very well established.⁵⁻⁷ The advantage of the observed two-dimensional growth mode of MgO on Fe is the possibility of obtaining a high quality ultrathin layer without pinholes and with a very flat surface. Consequently, a very small coupling is observed. The quality of the MgO barrier in Fe/MgO/Fe system grown on Fe whiskers has been characterized locally by Wulfhekel *et al.*,⁷ and most of the tested area was found to have intrinsic tunneling properties corresponding to a good insulating MgO barrier. Single crystalline systems Fe/MgO/Fe₅₀Co₅₀ have also been deposited on semiconductor GaAs substrates by Martinez Boubeta *et al.*,⁸ with a MgO insulating layer down to 2 nm. These junctions with a diam-

eter of 10 μm , prepared by sputtering and laser ablation, showed a TMR ratio of 27% at room temperature.⁹

In epitaxial systems, magnetic anisotropy is driven by the crystalline structure. Hence, the magnetic rigidity of both magnetic subsystems can be controlled with the purpose of obtaining of a very flat TMR plateau region. Moreover, the presence of the crystalline anisotropy in the magnetic layers will prevent the creation of magnetic inhomogeneities in the electrodes, known to have detrimental effects on the magnetotransport properties of the MTJ devices, as has already been mentioned¹⁰ in case of polycrystalline sputter-grown systems (loss in signal, magnetostatic coupling effects, etc.).

For our studies, we have used MBE with a base pressure of 2×10^{-11} Torr. After annealing the MgO substrate at 500 °C for 20 min, first a 50-nm-thick Fe layer was deposited using a Knudsen cell at 0.7 nm/min. The iron layer grows pseudomorphically on MgO(100) substrate, and the lattice mismatch is 3.7% when the Fe unit cell is turned by 45° with regard to the MgO unit cell. To improve the surface quality, the Fe layer was annealed at 450 °C for 15 min. The surface rms roughness after annealing, estimated from atomic force microscope images, was about 0.3 nm. A thin MgO insulating layer was subsequently deposited by means of an electron gun at 0.5 nm/min. We found that insulating barriers of thickness from 0.5 to 3 nm grew epitaxially on the Fe layer. Two-dimensional layer-by-layer growth^{6,11} was observed up to several monolayers by means of reflecting high energy electron diffraction (RHEED) intensity oscillations (Fig. 1) and the in-plane lattice parameter oscillations. The second magnetic 5-nm-thick Fe layer was epitaxially grown on the top of the insulating MgO barrier. Then, a Co layer with thickness of 50 nm was deposited on the top of iron using electron gun at 3 nm/min. RHEED images indicate clearly an epitaxial growth of Co on Fe. To prevent the *ex-situ* oxidation of the top Co layer and to protect it during the subse-

^{a)}Electronic mail: popova@lpm.u-nancy.fr

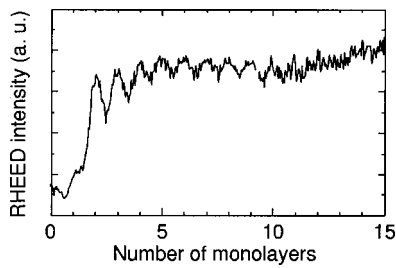


FIG. 1. RHEED intensity oscillations of MgO deposited onto the 50-nm-thick Fe buffer as a function of the number of monolayers.

quent patterning steps of the lithography, we have used a 10-nm-thick Pd capping layer.

Using a CM30/ST microscope whose point resolution is 0.19 nm, transmission electron microscopy (TEM) studies were performed on MgO(100)/Fe/MgO/Fe/Co/Pd MTJ with MgO barrier thickness from 0.8 to 2.5 nm. The cross-sectional specimens were cut along (100) MgO planes. The micrograph in the Fig. 2(a) is a dark field image of the sample with a 0.8-nm-thick MgO barrier, studied in cross section and acquired selecting the 002-MgO reflection. The bright contrasts therefore correspond to the oxide film, the substrate, and also to the Pd cap layer whose d-002 interreticular distance is very close to the MgO one. This image evidences the continuity of the MgO barrier at least over 0.3 μm (the image size). Similar microstructures were obtained for thicker barriers. The high resolution TEM (HRTEM) image in Fig. 2(b) shows the fine structure of the Fe/MgO/Fe/Co stacking sequence with a 0.8-nm-thick MgO barrier. In agreement with the RHEED experiments, the epitaxial relation between iron and magnesium oxide is Fe(001)

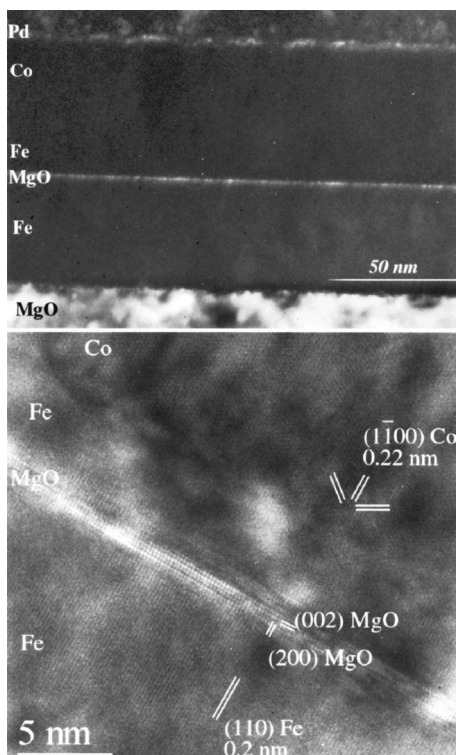


FIG. 2. TEM views of MgO(100)/Fe/MgO/Fe/Co/Pd multilayer with 0.8 nm MgO barrier: (a) cross-sectional 002 dark field image and (b) HRTEM micrograph.

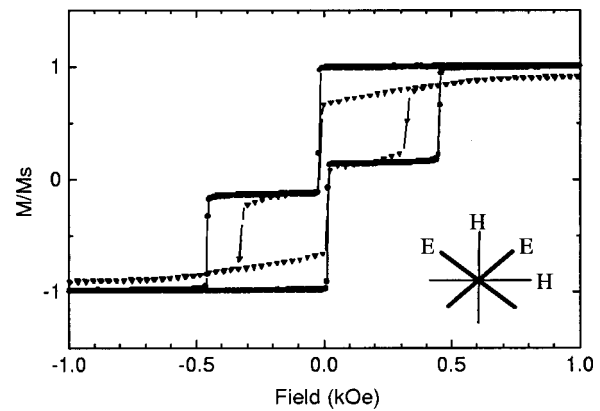


FIG. 3. Normalized magnetization curves $M-H$, measured along the easy (E \rightarrow) and hard (H \rightarrow) axis of a MgO(100)/Fe/MgO-1 nm/Fe/Co/Pd MTJ stack before lithography. M_S represents the saturation magnetization of the sample. The inset illustrates the alternating H/E axis.

$\times[110]\parallel\text{MgO}(001)[100]$ as in Ref. 6. For MgO thickness of 0.8 nm, no misfit dislocations were observed, whereas they were evidenced for thicker barriers. This result is in perfect agreement with the results of Vassent *et al.*⁶

The Fe/MgO/Fe interfaces are quite smooth with a roughness less than two (002) MgO planes (i.e., 0.4 nm). The Fe/Co interface is, however, quite rough as evidenced in the HRTEM micrograph in Fig. 2(b). In agreement with the RHEED analysis and x-ray diffraction measurements carried on onto the MTJ with 50-nm-thick Co film, the HRTEM experiments indicate a hexagonal compact packed (hcp) lattice for the cobalt layer, its sixfold axis being aligned along either the [100] or the [010] MgO direction. Therefore, two Co variants appear with the following epitaxial relation with respect to Fe: $\text{Co}(11-20)[0001]\parallel\text{Fe}(001)[110]$ and $\text{Co}(11-20)[0001]\parallel\text{Fe}(001)[1-10]$.

The tunneling probability of electrons, hence the resistance of MTJ, is controlled by the relative orientation of the magnetization of its ferromagnetic electrodes. The field window ($H_S < H < H_H$) between these two extreme resistance states is determined by the difference in the reversal fields of the two magnetic electrodes (H_H for the hard electrode and H_S for the soft electrode, respectively).

The magnetic properties have been investigated by magnetization versus field $M(H)$ loops, performed on continuous films with barrier thicknesses from 0.8 to 2.5 nm. As illustrated by Fig. 3, the bottom Fe layer has a low coercive field ($H_S \sim 20$ Oe) and a very sharp reversal along the easy magnetic axis. This bcc-Fe layer presents a fourfold in-plane symmetry. The hard bilayer Fe/Co, epitaxially grown on the MgO insulating barrier, presents a high coercive field $H_H > 400$ Oe and a sharp magnetization reversal. It presents also a fourfold symmetry with alternating hard and easy axis at 45° , directly related to the crystallographic structure of both bcc-Fe and hcp-Co constituting layers. We mention that the easy (hard) axis of the hard bilayer coincides with the easy (hard) axis of the soft layer. As we can clearly see in Fig. 3, along the easy axis of the hard layer, the plateau is very flat. Magnetic coupling has been deduced from minor $M(H)$ loops. For the all set of samples, the coupling is found to be very small, i.e., lower than 4 Oe.

In order to check their electrical quality, insulating layers

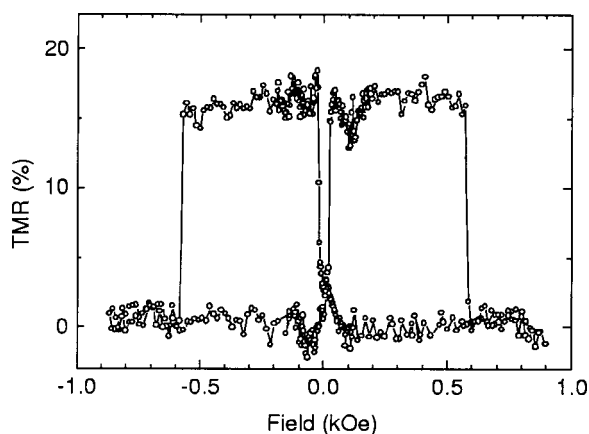


FIG. 4. Room temperature TMR of a $200\ \mu\text{m} \times 100\ \mu\text{m}$ large MgO(100)/Fe/MgO-1 nm/Fe/Co/Pd junction. The measurement is performed along the easy axis, the junction being biased at 10 mV.

have been tested using local impedance measurements.¹² For these measurements, we have grown Fe/MgO structures without the top Fe/Co electrode. For all the samples, with MgO thicknesses between 0.8 and 2.5 nm, the current flow was found to be very homogeneous. The current distribution was narrow (restricted to one decade) and could be fitted using a barrier fluctuation parameter¹² $\sigma < 1\ \text{\AA}$. Moreover, the tunnel current maps have shown that the insulator was hot-spot free over the scan area of micrometer size.

Next, the complete MTJ structures with lateral sizes between 20 and $200\ \mu\text{m}$ were designed using UV-lithography patterning.¹³ Large TMR signals have been measured on junctions of different lateral size. For a $200\ \mu\text{m} \times 100\ \mu\text{m}$ junction, with a 1-nm-thick MgO tunnel barrier, we observe a net TMR signal of about 15% at room temperature, with a flat plateau and a large operational field window (Fig. 4). The measured resistance of this junction is $4\ \text{k}\Omega\ \mu\text{m}^2$. This would correspond to a barrier height of 1.35 eV, estimated within the tunneling model of Brinkmann. *Ab-initio* calculations of Butler *et al.*¹⁴ predicted for Fe(100)/MgO(100) a theoretical gap of 5.5 eV which would roughly correspond to a barrier height above 2 eV, as the height is determined by the Fermi level position in the gap. However, our experimental barrier height is smaller as it reflects the integration of the barrier parameters over a large junction area.

Lower resistances have already been reported for MTJ with AlO_x barriers.^{2,15} However, the growth and the oxida-

tion of an ultrathin Al layer, deposited on top of the ferromagnetic film having a high oxygen affinity, are extremely difficult to control. On the contrary, the high quality two-dimensional MgO growth and low interlayer coupling field should allow a deposition of the MTJ with the spacer thinner than 0.8 nm and consequently, further reducing of the MTJ resistance.

In conclusion, we have shown that MBE can be used to control the growth of a very flat insulating layer with thickness below 1 nm, between two magnetic electrodes. Very low magnetic coupling, low resistance, and finally high tunnel magnetoresistance make this system an interesting model for the submicrometric MRAM.

The authors are grateful to G. Marchal for his ingenious conception of the MBE system, and to S. Robert for the x-ray diffraction measurements. This work was supported by the Nanomem Program (IST-1999-13741).

- ¹J. M. Daughton, J. Appl. Phys. **81**, 3758 (1997); W. J. Gallagher, J. H. Kaufman, S. S. P. Parkin, and R. E. Scheuerlein, US Patent No. 5,640,343 (17 June 1997).
- ²J. J. Sun, K. Shimazawa, and N. Kasahara, Appl. Phys. Lett. **76**, 2424 (2000).
- ³J. J. Sun, V. Soares, and P. P. Freitas, Appl. Phys. Lett. **74**, 448 (1999).
- ⁴C. Tiusan, M. Hehn, K. Ounadjela, Y. Henry, J. Hommet, C. Meny, H. A. M. van der Berg, L. Baer, and R. Kinder, J. Appl. Phys. **85**, 5276 (1999).
- ⁵T. Urano and T. Kanaji, J. Phys. Soc. Jpn. **57**, 3403 (1988).
- ⁶J. L. Vassent, M. Dynna, A. Marty, B. Gilles, and G. Patrat, J. Appl. Phys. **80**, 5727 (1996).
- ⁷W. Wulfhekel, M. Klaua, D. Ullmann, F. Zavaliche, J. Kirschner, R. Urban, T. Monchesky, and B. Heinrich, Appl. Phys. Lett. **78**, 509 (2001).
- ⁸C. Martinez Boubeta, E. Navarro, A. Cebollada, F. Briones, F. Peiró, and A. Cornet, J. Cryst. Growth **226**, 223 (2001).
- ⁹M. Bowen, V. Cros, F. Petroff, A. Fert, C. Martinez Boubeta, J. L. Costa-Krämer, J. V. Anguita, A. Cebollada, F. Briones, J. M. de Teresa, L. Morrellón, M. R. Ibarra, F. Güell, F. Peiró, and A. Cornet, Appl. Phys. Lett. **79**, 1655 (2001).
- ¹⁰C. Tiusan, T. Dimopoulos, L. Buda, V. Da Costa, K. Ounadjela, M. Hehn, and H. van den Berg, J. Appl. Phys. **89**, 6811 (2001).
- ¹¹P. Turban, L. Hennes, and S. Andrieu, Surf. Sci. **446**, 241 (2000).
- ¹²V. Da Costa, C. Tiusan, T. Dimopoulos, and K. Ounadjela, Phys. Rev. Lett. **85**, 876 (2000).
- ¹³F. Montaigne, PhD thesis, University Paris VII (1999).
- ¹⁴W. H. Butler, X.-G. Zhang, T. C. Schulthess, J. M. MacLaren, Phys. Rev. B **63**, 054416 (2001).
- ¹⁵S. S. P. Parkin, K. P. Roche, M. G. Samant, P. M. Rice, R. B. Beyers, R. E. Scheuerlein, E. J. O'Sullivan, S. L. Brown, J. Bucchigano, D. W. Abraham, Y. Lu, M. Rooks, P. L. Trouilloud, R. A. Wanner, and W. J. Gallagher, J. Appl. Phys. **85**, 5828 (1999).